INTERNATIONAL JOURNAL OF CURRENT RESEARCH IN CHEMISTRY AND PHARMACEUTICAL SCIENCES

(p-ISSN: 2348-5213: e-ISSN: 2348-5221)
www.ijcrcps.com

Research Article

SUPERPARAMAGNETIC Fe_3O_4 NANOPARTICLES FOR MAGNETIC FLUID HYPERTHERMIA: HIGH SPECIFIC ABSORPTION RATE (SAR) AND NEED FOR REDUCED INTERPARTICLE MAGNETIC INTERACTION

NINGOMBAM GOUTAM SINGH AND NONGMAITHEM RAJMUHON SINGH*

Department of Chemistry, Manipur University, Canchipur – 795003, Manipur, India.
Corresponding Author: nrajmuhon@manipuruniv.ac.in

Abstract

Surface modified superparamagneticFe_3O_4 nanoparticles were prepared by alkaline co-precipitation of water soluble Fe(II) and Fe(III) salts.Fe_3O_4nanoparticles were surface modified with folic acid (FA) and ascorbic acid (AA).Samples were characterized by X-ray diffractometry, transmission electron microscopy, fourier transform infrared spectroscopy, thermogravimetry, vibrating sample magnetometry and induction heating study. X-ray diffractometry study has shown that the samples crystallize into a single cubic phase with a = b = c = 8.396±0.03 Å.The synthesized nanoparticles have maximum probable average size of 10 – 12 nm. The nanoparticles prepared in presence of ascorbic acid was found to have more uniform particle and size distribution. The sufficiently high magnetization, induction heating abilities, high specific absorption rate (SAR) values and cell viability profiles on HeLa cells opened a scope for further *in vivo* study for cancer hyperthermia applications. The study observed that particle size and shape, reduced interparticle magnetic interactions and surface modification are necessary for practical applicability

Keywords: Iron oxide; hyperthermia; ascorbic acid; folic acid; magnetic interaction; specific absorption rate.

Introduction

Functionalized magnetic nanoparticles have become one of the most important inorganic nanoparticles pursued by the researchers for biomedical applications. Superparamagnetic iron oxide nanoparticles have been extensively used for drug delivery (Hari, 2009; Rui, 2009;),magnetic fluid hyperthermia(Andreas, 1993; Veronica, 2009),gene delivery (Dobson, 2006), magnetic resonance imaging (Kumar et al. 2012; Hyon et al., 2009),biosensors (Kavitha et al., 2013), tissue engineering (Ito and Kamihira, 2011), in vivo cell monitoring(Bulte, 2004)due to their favourable magnetic properties, biocompatibility, chemical stability over physiological circumstances and substantial accumulation at the diseased site.

For cancer hyperthermia, superparamagnetic iron oxide nanoparticles is becoming a very potential material because of its ability to mediate heat induction under an alternating current magnetic field. Superparamagnetic Fe_3O_4 ferrofluids (suspensions in suitable liquids) generates thermal energy predominantly via the relaxation in their magnetic moments (Runa, 2011; Rosensweig, 2002). The heat energy dissipation leads to a localized temperature rise which can cause destruction of cancer cells since cancerous tissues are more sensitive to heat than the normal tissues(Andreas et al., 1993). Gordon et al. suggested that intracellular hyperthermia would be an effective approach towards cancer therapy compared to extracellular hyperthermia since the cell membrane could act as thermal insulator(Gordon, 1979). When the rate of heat loss by conduction exceeds the heat dissipation by magnetic particles, the heating effect induced to the cell would be negligible thereby limiting the utility of magnetic fluid hyperthermia (Rabin, 2002). Therefore, it is necessary to deliver and accumulate the magnetic nanoparticles in the vicinity of cancer cells. The delivery of these magnetic nanoparticles to a specific site of interest can

be achieved by the application of a static magnetic field in the vicinity. The ease of remote controlling the magnetic nanoparticles to cause generation of thermal energy by the application of alternating magnetic field facilitates the controlled drug release or selective destruction of cancerous tissues.

However, hydrophobicity, magnetic dipolar interactions and van der Waals attraction often cause aggregation of magnetic nanoparticles in suspension leading which limits the application. Surface modification of magnetic nanoparticles with biocompatible and biodegradable molecules to enhance their solubility and stability in suspensions is indispensable for biomedical applications (Morteza et al., 2011).The retention of nanoparticles in cancer cells can be enhanced by active targeting to cell membrane receptors over-expressed in cancer cells. Folate receptors of folate binding proteins are highly expressed in a number of human epithelial carcinomas however with limited expression on normal cells (Steven et al., 1992; John, 1994: Nikki, 2005;Chun, 2003), Such over-expression of folate receptors are also observed in breast, colorectal, renal and lung cancer though at lower frequencies (20%-50%). Human ovarian and endometrial cancers have high probability of expression of high affinity receptors which do not show in normal cells. Activated and non-resting macrophages have also been found to express the folate receptors. Since folic acid is essential for methylation and DNA synthesis in cellular processes (Stanger, 2002), it could also serve as facilitator for tumour cell proliferation. Besides, the cheap availability, small size of the ligand, suitability to various tumours and ease of cytosolic uptake via receptor mediated endocytosis(Rohidas et al., 2010: Kumar et al., 2012) have added to the advantage of folic acid as ligand for surface modification and tumor targeting. Ascorbic acid is known to have certain positive effects including reducing risks of cancer in mouth and breast, osteoarthritis, HIV transmissions, etc. .(http://www.webmd.com) Ingredient mono-1001-Vitamin C (VITAMIN C (ASCORBIC ACID)).aspx). It is helpful in increasing the absorption of iron from foods and proper immune function. Cancerous cells also collect high concentrations of ascorbic acid.

In this article, we have shown the preparation method for surface modified Fe_3O_4 magnetic nanoparticles (MNPs). Folic acid (FA) and ascorbic acid (AA) are used as surface modification ligands so that bio-compatible particles can be targeted in cancer cells in physiological conditions. Their efficiency towards the production of high absorption rate (SAR) is discussed.

Materials and Methods

Preparation of iron oxide nanoparticles

Anhydrous ferric chloride ($FeCl_3$, Merck) ferrous sulphate heptahydrate ($FeSO_4.7H_2O$, Himedia), ammonium hydroxide (NH_4OH, Merck), L-ascorbic acid ($C_6H_8O_6$, Himedia), folic acid (Himedia) were used for the preparation of samples. Typically, a mixture of 20mL of 0.25 M $FeSO_4.7H_2O$ solution and 40mL of 0.25 M $FeCl_3$solution were taken together and warmed to 60 ^oC. under vigorous stirring, 60mL of 10M NH_4OH was added to the mixture when precipitates appeared immediately. After stirring continued for 2h, the black precipitates were concentrated by magnetic decantation and the supernatant liquid was partially removed to keep the medium still alkaline. For each surface modification step, the Fe_3O_4 nanoparticles were prepared freshly.

Surface modification with folic acid (Fe_3O_4@FA) and ascorbic acid (Fe_3O_4@AA)

For surface modification with folic acid (FA), firstly 1g of FA was dissolved in 50 mL of water-methanol (4:1 v/v) mixture. The dissolved FA was added to the concentrated Fe_3O_4 precipitate in a beaker. The whole mixture was ultrasonicated for 2h and kept standing overnight (12h) at 40^{o}C. The product was separated by magnetic separation while washing with distilled water and ethanol twice. The black mass was dried at 60^{o}C for 6h for further analysis. Similarly for surface modification with ascorbic acid (AA), 1g of AA was dissolved in 50 mL of water-methanol (4:1 v/v) mixture and followedthe same procedure as stated above.

Characterization

The prepared samples were studied for phase purity and crystal structure using PANalytical powder X-ray diffractometer (X'-PertPRO) with CuKα (1.5406 Å) radiation and Ni filter. The powdered sample of Fe_3O_4 was placed in the sample container and it was mounted at the sample holder. The X-ray tube was operated at 20 mA and 40 kV. The X-ray diffraction (XRD) pattern was recorded at step size of 0.03^o/s in 2θ. Unit cell parameters were calculated using UnitCell Program © Tim Holland and Simon Redfern. Average crystallite sizes of particles were calculated by the well-known Scherrer formula, $d = 0.9\lambda/\beta\cos\theta$ where $d$is the mean crystallite size; λ, the X-ray wavelength; β, the full width at half maximum of highest intensity peak; and θ, the Bragg's diffraction angle.

Transmission electron microscope (TEM, JEOL JEM-2100, Japan) was used to record the shape and size of the iron oxide samples. For this, the powder magnetic nanoparticles were dispersed in methanol under ultrasonic vibration for 1h. A drop of the dispersed particles was put over the carbon coated copper grid and evaporated to dryness at room temperature. It was mounted inside the sample chamber. The interaction of surface modifying ligands – folic acid and ascorbic acid – with Fe_3O_4 was characterized by Fourier Transform

Infrared (FT-IR) Spectroscopy (Shimadzu FT-IR 8400S) with a resolution of 4 cm^{-1}. FT-IR spectra were recorded using thin pellets of the samples made with KBr. Thermogravimetric analysis(TGA) was performed in a flushing nitrogen atmosphere by Pyris Diamond TGA/DTA(Perkin Elmer) to determine the amount of Fe_3O_4 in the surface modified nanoparticles. Magnetization measurements of functionalized iron oxide samples was carried out at room temperature (300K) using Vibrating Sample Magnetometer (Lakeshore VSM 7410, USA).

Hyperthermia study

The measurements of the induction heating ability of the magnetic nanoparticles (MNPs) were performed using Easy Heat 8310, Ambrell, UK. The instrument was equipped with induction coil of 4 turns with diameter of 6cm, operating frequency 265 kHz and the provision of water circulation through their coils in order to keep ambient temperature. Sample suspended in 1mL of deionised water was taken in 1.5mL micro-centrifuge tube and this was placed at centre of the coil without touching the walls. The sample was heated using current of 200 A, 300 A and400 A up to 10 minutes (600 seconds). The resultant magnetic field (H) generated due to the applied current (i) was calculated by making use of the following relation:

$$H = \frac{1.257ni}{L} \text{ (in Oe)}$$

where n, number of turns in coil and L, diameter of turn in cm. The calculated values of the magnetic fields with respect to the applied currents of 200, 300 and 400 A were 168, 251 and 335 Oe (equivalent to 13, 20 and 27 kAm^{-1}), respectively. The temperature of the system, where the sample was kept in the centre of the coil was recorded using an optical temperature sensor (Photon R & D, Canada) with the accuracy of ±0.01 °C.

Cell line and culture

The detailed toxicity profiles of the surface modified iron oxide nanopartilces were studied on Human Epitheloid Cervix Carcinoma (HeLa) cell line by MTT [(3-(4,5-dimethylthiazol-2-yl)-2,5-diphenyl tetrazolium bromide] assay. HeLa cell line was obtained from the National Centre for Cell Sciences, Pune, India. The HeLa cells were grown in DMEM (Dulbecco's Modified Eagle Medium) supplemented with 10%(v/v) fetal bovine serum and penicillin G (100 U/mL) at 37 °C in a 5% CO_2 atmosphere.

***In-vitro* cell viability**

Cell viability studies were performed on the HeLa cell lines using MTT assay. The cells were incubated with the concentration of 1× 10^6 cells mL^{-1} in the respective medium for 24h in a 96-well microtire plate. After 24 h the old media was replaced by fresh media and different proportions of sterile iron oxide magnetic particles (0.2, 0.5, 1.0, 1.5 and 2 mg mL^{-1} of cultured media) were added. Then the total medium was incubated at 37 °C in a 5% CO_2 atmosphere for 24h. After incubation of iron oxide treated cells for 24h, 10 µL MTT solution was added into each well including control wells. The plates were incubated for 3h at37 °C in a 5% CO_2 atmosphere for metabolization of MTT with the nanoparticles and cell media. Then, the total medium was removed by flicking the plates and only anchored cells remained in the wells. The cells were then washed with phosphate buffer saline (PBS) and any formazan formed was extracted in 200 µL acidic isopropanol and finally the absorbance is read at 570 nm and from it the cell viability was calculated. The experiments were replicated three times and the data was graphically presented as the mean. The cell viability was calculated by:

$$\% \text{ Cell viability} = \frac{\text{Absorbanceofsamplewell}}{\text{Absorbanceofcontrolwell}} \text{ X } 100$$

Results and Discussion

XRD study

Figure 1 showed the XRD pattern of functionalized iron oxide nanoparticles (Fe_3O_4@FA and Fe_3O_4@AA) which conform to the reference JCPDS 85-1436. The patterns indicated crystalline single phase nanocrystals with a face-centred cubic structure and a space group Fd3m. The lattice parameters of Fe_3O_4@FA and Fe_3O_4@AA are calculated to be a = b = c = 8.396±0.03 Å.The average crystallite sizes are calculated to be 11.4, 10.3 and 11.0 nm respectively for Fe_3O_4,Fe_3O_4@FA and Fe_3O_4@AA.

FT-IR study

Figure 2 shows the FT-IR spectra of ascorbic acid (AA) and Fe_3O_4@AA nanoparticles. Ascorbic acid (AA) has several vibrational peaks corresponding to C – C stretching (850-1000 cm^{-1}), C – O stretching (1115cm^{-1}), CH_2 deformation (1395 cm^{-1}, 1438 cm^{-1} 1516 cm^{-1}), C – O symmetric stretching (1338 cm^{-1}), C = C stretching (1652 cm^{-1}), C = O stretching (1754 cm^{-1})and the O – H stretching (3050 cm^{-1}, 3212 cm^{-1}, 3318 cm^{-1}, 3412 cm^{-1}, 3525 cm^{-1})(Jan and Peter, 1971). In the FT-IR spectra of Fe_3O_4@AA nanoparticles, the O – H stretching bands in 3035-3600 cm^{-1} of AA are missing. Instead, a broad band with peak 3452 cm^{-1} is observed. In AA, C = O(1754 cm^{-1}) is observed, but this is missing in Fe_3O_4@AA. Instead, a broad band at 1672 cm^{-1} has been observed. It may be due to interaction of C = O and O-H groups of AA with Fe^{2+}/Fe^{3+} of Fe_3O_4. The broad peak at 600cm^{-1} is observed and this is assigned to Fe – O.

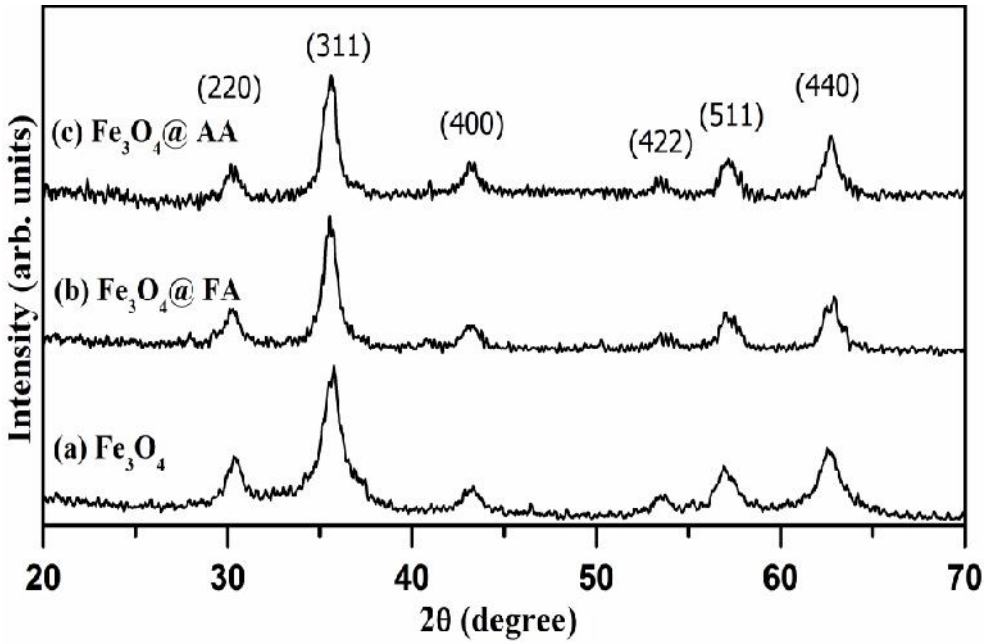

Fig. 1. XRD patterns of (a) bare Fe_3O_4(b) Fe_3O_4@FA and (c) Fe_3O_4@AA nanoparticles.

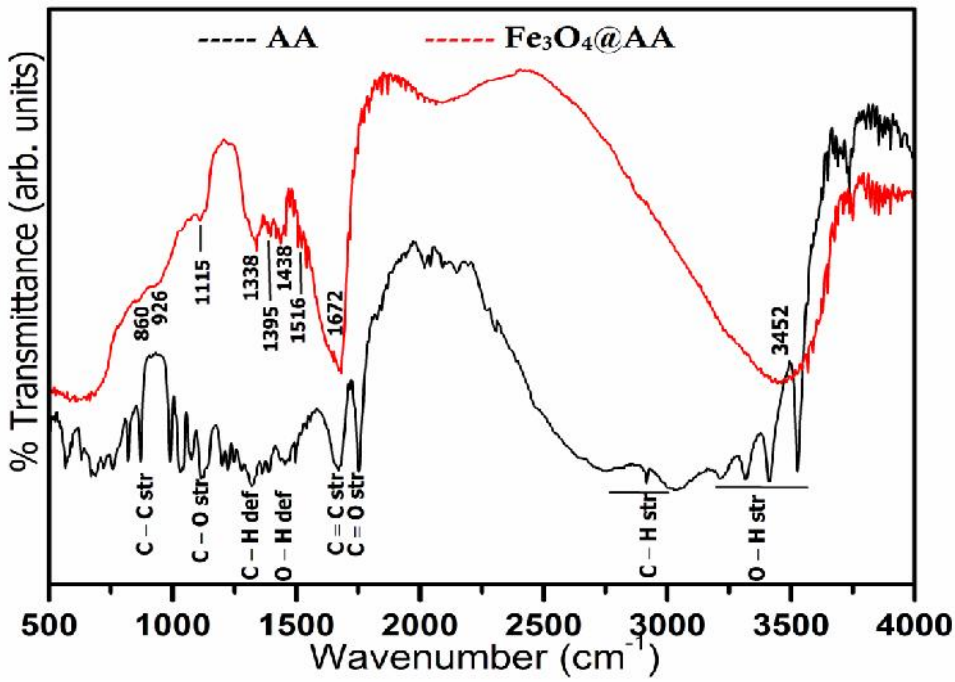

Fig. 2. FTIR spectra of commercial ascorbic acid (AA) and functionalized iron oxide nanoparticles (Fe_3O_4@AA).

Figure 3 shows the FT-IR spectra of folic acid (FA) and Fe_3O_4@FA nanoparticles. Folic acid (FA) has several vibrational peaks corresponding to C – C stretching (850-1000 cm^{-1}), C – N stretching (1190 cm^{-1}), C – O symmetric stretching (1224 cm^{-1}, 1338cm^{-1}), C = C ring stretch (1458 cm^{-1}), – CH_2 deformation (1390 cm^{-1}, 1516 cm^{-1}), N – H deformation (Amide II, 1543 cm^{-1}), C = O stretching (Amide I, 1636 cm^{-1}), C – H stretching (sym, 2839 cm^{-1} and asym, 2932cm^{-1}), N – H stretching (3120 cm^{-1} and 3323 cm^{-1})and O – H stretching (3415 cm^{-1} and 3552 cm^{-1}) (Sonali et al., 2010; Silverstein et al., 2005).

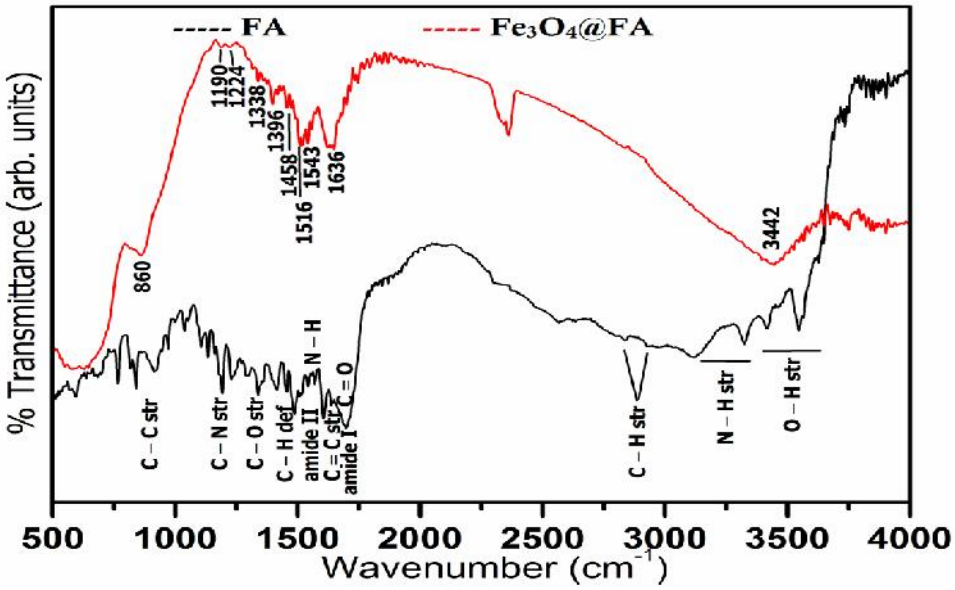

Fig. 3. FTIR spectra of commercial folic acid (FA) and functionalized iron oxide nanoparticles (Fe_3O_4@FA).

In the FTIR spectra of Fe_3O_4@FA, the N – H stretching band at ~ 3300 cm^{-1} is merged with broad peak of O – H stretching band. COOH and NH_2 groups are engaged in interaction with Fe_3O_4. Thus a broad peak with maximum at 3442 cm^{-1} appeared. The peaks at 1516 and 1636 cm^{-1}suggests interaction between $–COO^-$group of FA and Fe^{3+}/Fe^{2+} of Fe_3O_4.The $–COO^-$can have two symmetric stretching vibrations. A broad peak at 600 cm^{-1} is assigned to Fe – O.The FT-IR observations have proved the successful surface modification of iron oxide nanoparticles.

TGA study

Thermogravimetric analysis was performed to quantify the amount of ascorbic acid and folic acid adsorbed on the surface of Fe_3O_4 nanoparticles. Figure 4 shows the thermogravimetric curves of Fe_3O_4@AA and Fe_3O_4@FA nanoparticles obtained in temperature range of 40 to 1000°C. In all the samples, abrupt weight loss is observed upto about 300°C. The decrease in weights in the region of 40 – 300°C of the thermograms could be attributed to loss of surface adsorbed water molecules, associated particles and decomposition of organic functionalized agents. While the gradual continuous decrease of weight from 300 – 600°C is due to loss of carbon residues. Thermograms have shown that the Fe_3O_4 contents of Fe_3O_4@AA and Fe_3O_4@FA nanoparticles are 86% and 93% respectively.

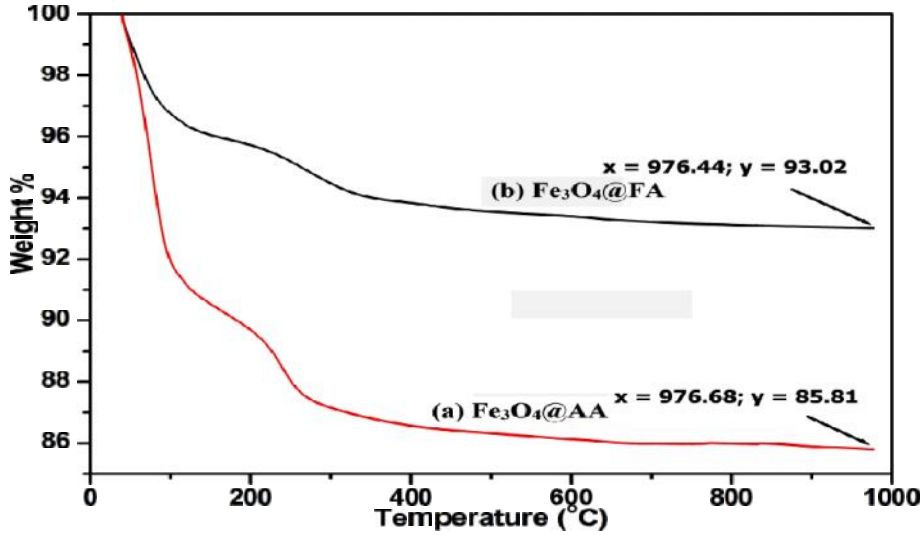

Fig. 4. Thermogravimetric curves of(a) Fe_3O_4@AA and (b) Fe_3O_4@FA nanoparticles obtained in temperature range of 40°C to 1000°C in an atmosphere of nitrogen.

Magnetization study

Figure 5 shows the magnetization of as-prepared surface modified iron oxide nanoparticles against the applied magnetic field strength. Since magnetization is found to be unsaturated till 1.5 X 10^4Oe, the saturation magnetization(M_S) is calculated from M vs. 1/H curve. The M_S values of the Fe_3O_4@FA and Fe_3O_4@AA are found to be 43.5emu/g and 33.0 emu/g respectively. The bulk Fe_3O_4 has a M_S value of 92 emu/g and coercivity (H_C) of 323 Oe (Cullity and Graham, 2009; Goya et al., 2003). All the samples showed negligible residual magnetization (0.03 – 0.4 emu/g) and coercivity (2-6 Oe) suggesting the superparamagnetic behavior of surface modified iron oxide nanoparticles. The low M_S values of functionalized iron oxide nanoparticles is due to increasing spin disorder on the nanoparticle surface which became more pronounced with decreasing size. Here, Fe_3O_4@FA has higher magnetization than Fe_3O_4@AA. It may be due to higher content of Fe_3O_4 per gram of powdered sample as given by TGA analysis.

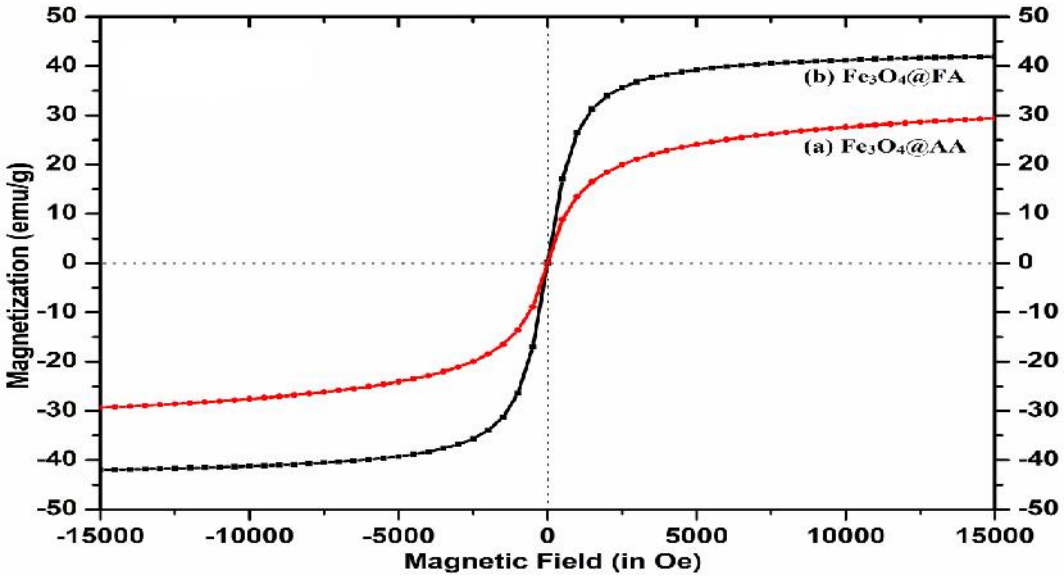

Fig. 5. Magnetization (M) versus applied magnetic field strength for (a) Fe_3O_4@AA and (b) Fe_3O_4@FA nanoparticles at 300K.

TEM Study

The TEM images of the surface modified nanoparticles of Fe_3O_4@AA and Fe_3O_4@FA are shown in Figures 6 (a) and (b) respectively. The nanoparticles are found to be more cubic in Fe_3O_4@AA and rather more spherical shape inFe_3O_4@FA. The Fe_3O_4@FA naoparticles appear to be a little agglomerated compared to Fe_3O_4@AA nanoparticles. The particle size distributions of Fe_3O_4@AA and Fe_3O_4@FA nanoparticles as obtained from TEM micrographs were shown in Figures 7 (a) and (b) respectively.

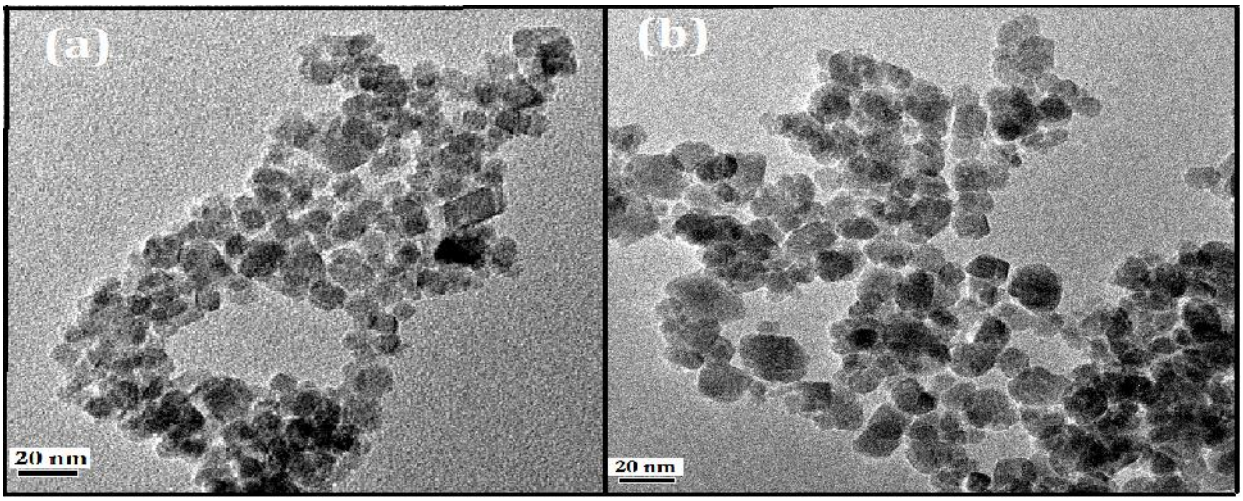

Fig. 6. TEM images of (a) Fe_3O_4@AA and (b) Fe_3O_4@FA nanoparticles.

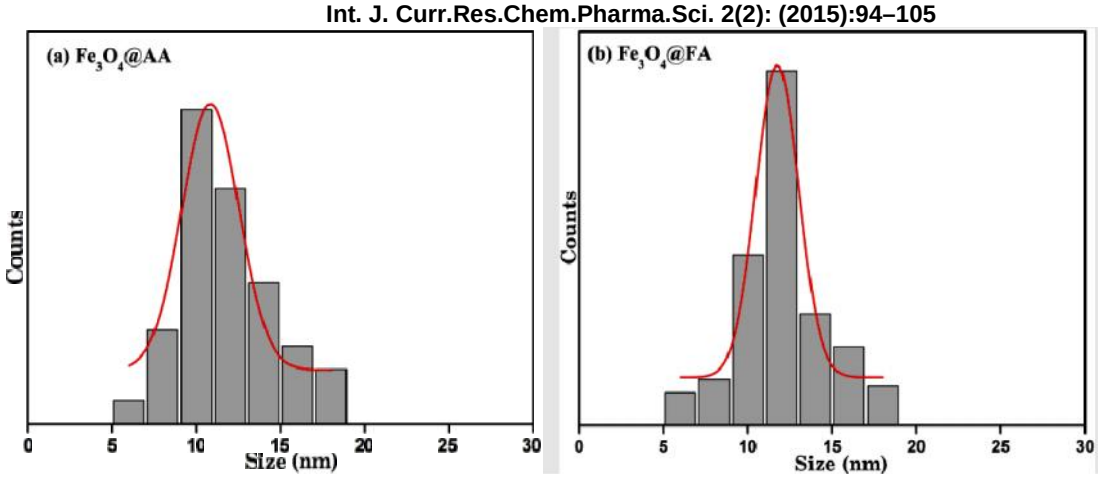

Fig. 7. The particle size distribution of (a) Fe_3O_4@AA and (b) Fe_3O_4@FA obtained from TEM micrographs.

The nanoparticles of Fe_3O_4@AA and Fe_3O_4@FA have sizes in the range of 5 – 20 nm with the maximum probable average size of 10 – 12 nm in the size distribution chart. The size obtained from the TEM images are found to be quite close to the sizes calculated from the XRD pattern of the nanoparticles. Fig. 8 showed the TEM, HRTEM and SAED patterns of the iron oxide nanoparticles. The HRTEM images indicate high crystalline packing of atoms in the nanocrystallites.The SAED patterns reveal lower crystallinity of Fe_3O_4@AA nanoparticles compared to Fe_3O_4@FA. The lower Fe_3O_4 content and lower crystallinity could have been a reason for lower M_S value of Fe_3O_4@AA. Particles having size less than 100 nm are favourable for specifically targeting the diseased site as they have reduced liver and kidney uptake and efficient cellular adhesion. Moreover, the particles below 100nm can evade reticulo-endothelial system and have sufficiently long blood circulation times (Ajay and Mona, 2005).

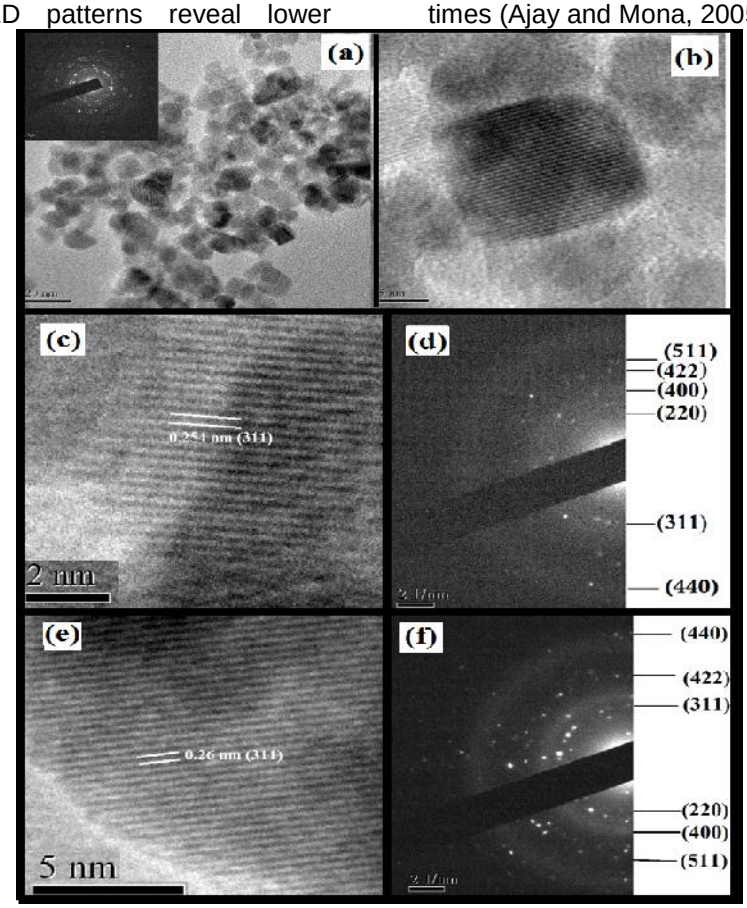

Fig. 8. TEM and HRTEM image of bare Fe_3O_4 nanoparticles (a & b) (inset: SAED pattern); HRTEM and SAED pattern of Fe_3O_4@AA (c & d); HRTEM and SAED pattern of Fe_3O_4@FA (e & f).

Induction heating ability of functionalized iron oxide nanoparticles

The induction heating measurements were carried out for surface modifiediron oxide nanoparticles under different current strengths (200A, 300A and 400A) for 10 min (600 seconds). For each sample, two sets of concentrations were studied. The magnetic nanoparticles suspension were prepared by dissolving 2mg and 5mg of magnetic nanoparticles in 1mL of distilled water. The heating ability of the magnetic nanoparticles was found dependent on its concentration and current applied. Time taken to raise the temperature becomes shorter with increasing current strength for each concentration. Substantially, an efficient heating rate was observed. Generally, for all samples, the current of 200 A was not sufficient to generate the hyperthermia temperature i.e. 41 – 46 ^{o}C.

For 2mg of Fe_3O_4@AA, (Fig. 9a) 300A and 400A were sufficient to generate the hyperthermia temperature. For 5mg of Fe_3O_4@AA, (Fig. 9b) the applied current strength – 200A, 300A and 400A – could be use to achieve the hyperthermia temperature. Therefore to achieve an efficient hyperthermia heat generation, the required concentrations of Fe_3O_4@AA nanoparticles were established as 2mg (@ 300A, 400A), 5mg (@ 200A, 300A and 400A). These results further suggest the advantage of current strength dose dependent application. 2mg at 300A and 400A may be highly beneficial for hyperthermia and temperature dependent target drug delivery which therefore will not cause thermal ablation of the cells and tissues in the vicinity of the target

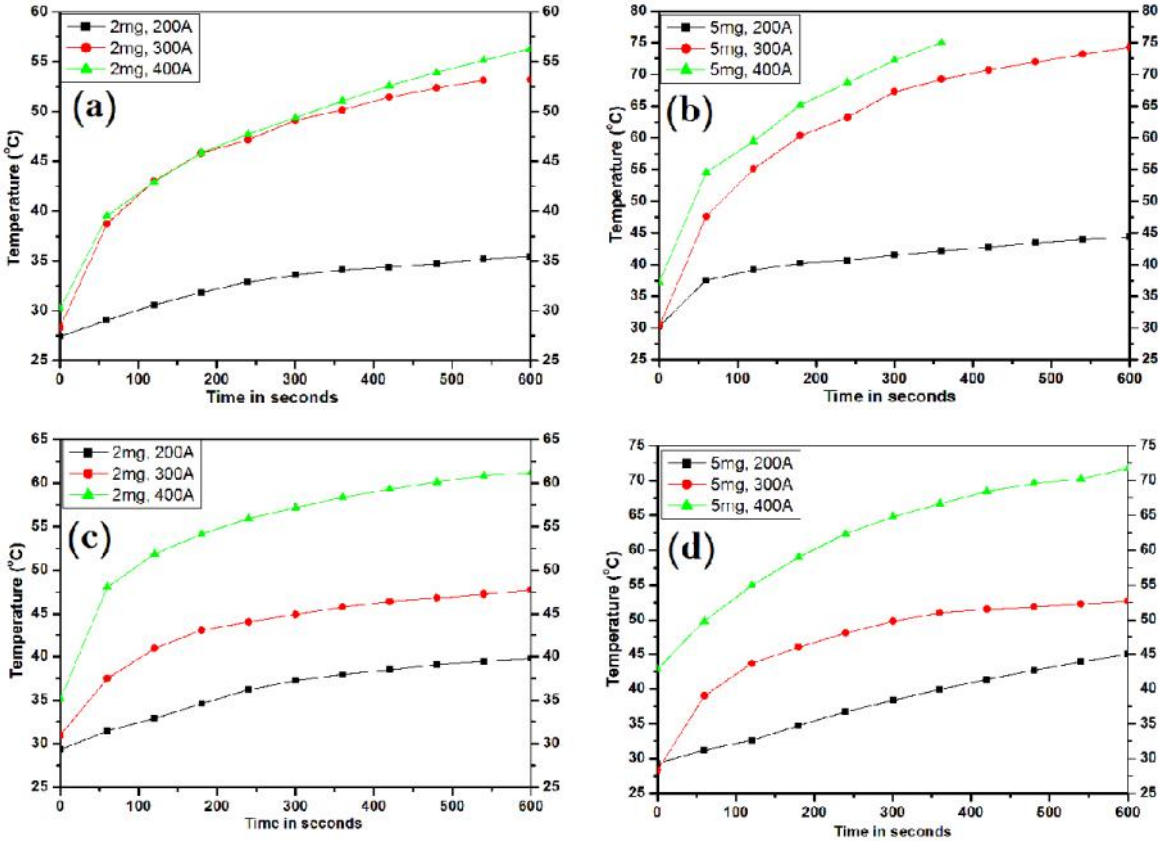

Fig. 9. Induction heating studies of (a, b) Fe_3O_4@AA, (c,d) Fe_3O_4@FA at different current strengths and different concentrations.

For Fe_3O_4@FA nanoparticles, 300A and 400A were found suitable in both concentrations – 2mg/mL (Fig. 8c) and 5 mg/mL(Fig. 8d) for hyperthemia heat generation. Hence, it is observed that even at low concentrations, the ferrofluids exhibited the hyperthermic temperature in short time at relatively low current strengths. Since the nanoparticlesbehave superparamagnetically, the main heat dissipation mechanismsof these nanoparticles are Neel and Brownian relaxation of magnetization moment(Goya et al., 2008).

The specific absorption rate (SAR), expressed in Wg^{-1} is used as the power of heating of a magnetic material per gram. The SAR values can be calculatedas a function of temperature gradient (dT/dt) by using the relation(Lee et al, 2011):

$$SAR = CV_s \frac{dT}{dt} \frac{1}{m_{mag}}$$

where C is the sample-specific heat capacity, V_s the sample volume, m_{mag} the mass of magnetic material in the sample. The sample-specific heat capacity is calculated as a mass weighted mean value of magnetite and water. Specific heats of Fe_3O_4 and water are 0.65 $Jg^{-1}K^{-1}$ and 4.18 $Jg^{-1}K^{-1}$ respectively. Since the concentration of magnetic materials in this case is very low, its contribution to the specific heat is negligible and hence the heat capacity for water is taken as the sample's heat capacity (Jun et al., 2008). The slope dT/dt of the time-dependent temperature curve is obtained from 0 – 240 seconds. Here the volume of water was 1mL, which is equal to 1g. The actual amount of Fe_3O_4 contained in the magnetic nanoparticles is obtained from the thermogravimetric (TGA) analysis. The SAR values of functionalized iron oxide nanoparticles at different current strengths are shown in Table 1. The heating efficiencies and SAR valuesare comparatively higher than the reports made earlier (Jun et al., 2008; Prasad et al., 2013; Zhang et al., 2007; Kim et al., 2008; Kita et al., 2008; Bilalis et al., 2012).

Table 1. Calculated Specific Absorption Rates of the functionalized iron oxide nanoparticles at different current strengths; the table also contains comparison with the previous reported values.

Sample Name	Current Strength in ampere [kA m^{-1}]#	SAR (Wg^{-1})	Reference
Fe_3O_4@AA	200 [13]	51	
	300 [20]	166	
	400 [27]	164	
Fe_3O_4@FA	200 [13]	64	
	300 [20]	122	
	400 [27]	194	
Fe_3O_4@Oleic Acid	400 [27]	33	Runa et al., 2011
Fe_3O_4@PEG		28	
Fe_3O_4	400 [27]	29	Prasad et al., 2013
Fe_3O_4(commercial)	*	85	Jun et al., 2008
Feridex nanoparticles		83	Bae et al., 2012

*The current strength was given to be 13kW.#The values in [ ] represents the current strength in kAm^{-1}

In the study, higher heating capacities are observed at lower concentrations of functionalized iron oxide nanoparticles. When a current strength of 400A is applied, Fe_3O_4@AA exhibited SAR values of 164 Wg^{-1} and 118 Wg^{-1} respectively for 2mg/mL and 5mg/mL suspension concentrations. And at 400A, Fe_3O_4@FA exhibited SAR values of 194 Wg^{-1} and 73 Wg^{-1} respectively for 2mg/mL and 5mg/mL suspension concentrations. At higher concentrations, there is a strong interparticle magnetic interactions which could lead to loss of magnetization energy via exchange interactions between the magnetic domains. When this magnetization energy has been compensated in such a manner, the heat generation upon relaxations of the magnetic domains will be reduced. Thus, reduced interparticle interaction amongst the magnetic nanoparticles is a must for efficient heat generation. Further, it was also observed that the Fe_3O_4@AA exhibited higher heating efficiency than the Fe_3O_4@FA. The TEM images showed the Fe_3O_4@AA nanoparticles have more uniform size and cubic shape compared to Fe_3O_4@FA. Hence, the size and shape and the reduced interparticle magnetic interactions are proved to be optimal conditions for efficient heat generation by magnetic nanoparticles

Cytotoxicity assay

The cytotoxicities of functionalized iron oxide nanoparticles are assessed by determining the viability of HeLa cell lines after incubation in a medium containing various concentration of nanoparticles for 24h (Fig. 10). The MTT assay measures the number and activity of living cells at the end of the assay. Thus, this assay is a very suitable method for cytotoxicity studies in mammalian cells as a measure of cell activation, cell growth and survival and to determine the chemosensitivity of cell lines(Mosmann, 1983). No significant cytotoxicity to the cells can be observed. The viability of this type of cells were >92%

for all the samples upto concentration of 1.5mg/mL. However, at 2mg/mLconcentration of nanoparticles, the viability decreases to about 80% for all the samples.This cytotoxicity profile suggest the biocompatibility of folic acid and ascorbic acid functionalized iron oxide nanoparticles.

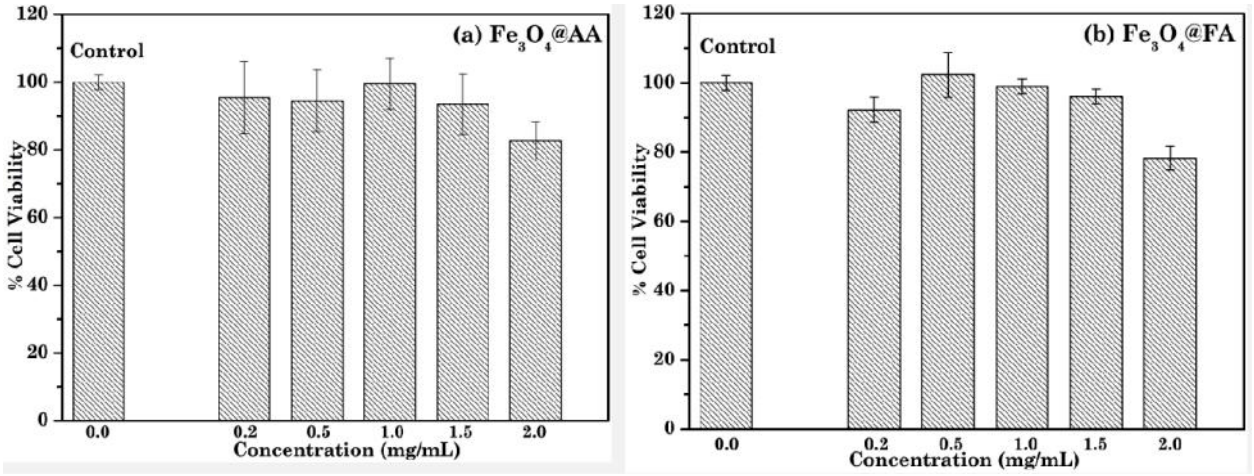

Fig. 10. Cell viability profile of HeLa cell lines as a function of (a) Fe_3O_4@AA (b) Fe_3O_4@FA nanoparticles concentration (0.2, 0.5, 1.0, 1.5 and 2.0 mg/mL) in the medium. The incubation period was 24h. Control cells without any treatment showed a viability of 100%.

This study demonstrates the better efficiency of magnetic Fe_3O_4ferrofluids used in our study for thermal killing of cancerous tissues. Despite small size of Fe_3O_4 nanoparticles, the ferrofluids observe high values of SAR, which is far better compared to previously reported. Moreover, though heat generation in alternating magnetic field is quite good, the magnetic metal and metal alloy nanopaticles such as Fe, Co, Ni, FePd, FePt, CoPt and CoPd have limitations because of their instability and high susceptibility to oxidation in slightly acidic and alkaline mediums similar to physiological conditions (Raghumani et al., 2012). Hence, the superiority of the functionalized Fe_3O_4 used in our study is proven. As our TEM results have shown that the Fe_3O_4@AAnanoparticles assumed rather more cubic structure and size less than 20nm. Ascorbic acid could be a better capping agent, owing to its reducing nature, that prevent the solubilisation of nanoparticles and hence Fe_3O_4@AA assumes more cubic shape. The size, shape and sufficiently high enough magnetization might have contributed to optimal anisotropy energy and morphology for efficient heatgeneration. These results indicate that optimal particle size and shape, reduced interparticle magnetic interactions and functionalization are necessary for practical applicability. Moreover, our reports have shown that the concentration required to achieve the hyperthermia temperature (i.e 41 – 46 ^oC) is as low as 2 mg/mL at an applied current strength of 300 A. This lowest ever reported dose for magnetic nanomaterials and alternating magnetic field would provide minimal invasiveness to the patient in the practical applications. The studies on the biocompatibility of the functionalized Fe_3O_4 nanoparticles revealed high cell viability. These observations might be associated with efficient cellular uptake and advances towards intracellular hyperthermia since cancerous tissues possess high affinity towards folic acid and ascorbic acid. Thus, this still opened the subject of furtherin vivo investigations.

Conclusion

This report presents an easy chemistry for surface modification of iron oxide nanoparticles with carboxylic groups. It clearly demonstrates the effect of surface functionalizations of iron oxide nanoparticles on the surface behavior, biocompatibility and induction heating abilities. The ascorbic and folic acid functionalization were found to have high heating efficiency. Even at low concentrations and low current strengths, these nanoparticles are favourable for efficient heat generation. The cytotoxicity profiles of the iron oxide nanoparticles on the HeLa (Human Epitheloid Cervix Carcinoma) cell line implies an applicability of these nanoparticles for induction heating therapy. The particle size as prepared were found to highly suitable for long blood circulation time and tissue diffusion. Besides optimal particle size, shape and surface modification, the study further observed that reduced interparticle magnetic interactions is also an indispensable factor for efficient heating. The results validated the extension of the studies to *in vivo* experimental models.

Acknowledgments

N. G. Singh would like to thank University Grants Commission, New Delhi for providing Senior Research Fellowship. N.R. Singh acknowledged Department of Biotechnology, New Delhi for granting financial assistance. We are grateful to Dr. Raghumani S.N., BARC for his guidance and assistance on hyperthermia facility. Also we express our gratefulness to SAIF, IIT Madras and SAIF, NEHU Shillong for VSM and TEM facility respectively; Physics Department, Manipur University for XRD facility; APT Research Foundation, Pune for Cell viability test.

References

Ajay K.G. and Mona G., 2005. Synthesis and surface engineering of iron oxide nanoparticles for biomedical applications. Biomaterials 26:3995-4022

Andreas J., Peter W., Horst F. John W., Hinz A.and Roland F., 1993. Inductive heating of ferrimagnetic particles and magnetic fluids: physical evaluation of their potential for hyperthermia. Int. J. Hyperthermia 9(1):51-68.

B. D. Cullity, C.D. Graham, Introduction to Magnetic Materials, second ed., A John Wiley & Sons, Inc., Publication, New Jersey, 2009.

Bae K.H., Mihyun P., Min J.D., Nohyun L., Ji H.R., Gun W.K., Cheol G.K., Tae G.P. and Hyeon T., 2012. Chitosan oligosaccharide stabilized ferromagnetic iron oxide nanocubes for magnetically modulated cancer hyperthermia. ACS Nano 6(6):5266-5273.

Bilalis P, Chatzipavlidis A., Tziveleka L.A., Boukos N., Kordas G., 2012. Nanodesigned magnetic polymer containers for dual stimuli actuated drug controlled release and magnetic hyperthermia mediation.J. Mater. Chem. 22:13451-13454.

Chun Y.K., Carla J. M. and Mark A.G., 2003. The folate receptor as a molecular target for tumor-selective radionuclide delivery. Nucl. Med. Biol. 30:811-817.

Dobson J., 2006. Gene therapy progress and prospects: magnetic nanoparticle-based gene delivery. Gene Therapy 13:283-287.

G.F. Goya, T.S. Berquo, F.C. Fonseca, M.P. Morales, 2003, Static and dynamic magnetic properties of spherical magnetite nanoparticles. J. Appl. Phys. 94:3520-3528.

G.F. Goya, V. Grazu, M.R. Ibarra, 2008. Magnetic nanoparticles for cancer therapy. Curr. Nanosci. 4:1-16

Hari K.S., Michael P. E., Hui M.,, Andrew Y. W., Shuming N. and Lily Y. 2009. Development of multifunctional nanoparticles for targeted drug delivery and non- invasive imaging of therapeutic effect. Curr. Drug Discovery Technol. 6(1):43-51.

Hyon B.N., In C.S., Taeghwan H., 2009. Inorganic nanoparticles for MRI contrast agents. Adv. Mater. 21:2133-2148.

http://www.webmd.com/vitamins-supplements/ingredientmono-1001-vitamin+c.aspx? active Ingredient Id=1001 &active Ingredient Name= vitamin +c & source=1, accessed on 23/11/2013).

Ito A. and Kamihira M., 2011. Tissue engineering using magnetite nanoparticles. Prog. Mol. Biol. Transl. Sci. 104:355-95.

J.H. Lee, J.T. Jang, J.S. Choi, S.H. Moon, S.H. Noh, J.W. Kim, J.G. Kim, I.S. Kim, K.I. Park, J. Cheon, 2011. Exchange-coupled magnetic nanoparticles for efficient heat induction. Nature Nanotechnology 6:418-422.

J.W. Bulte, D.L. Kraitchman, 2004. Iron oxide MR contrast agents for molecular and cellularimaging. NMR Biomed. 17:484-499.

Jan H. and Peter K., 1971. Vibrational spectroscopic studies of L-ascorbic acid and sodium ascorbate. Acta. Chem. Scand. 25:3043-3053

John F.R., Prabir K.C. and Manohar R., 1994. Differential Regulation of Folate Receptor Isoforms in Normal and Malignant Tissues In Vivo and in Established Cell Lines Cancer. 73:2432-2443.

Jun M., Toshiyuki H., Ryuji K., Noriyuki Y., Tomio M., Takeshi K. and Hiroyuki H., 2008. Size dependent heat generation of magnetite nanoparticles under AC magnetic field for cancer therapy. BioMagn. Res. Technol. 6:4.

Kavitha A.L., Prabu H.G., Babu S.A. and Suja S.K., 2013. Magnetite nanoparticles-chitosan composite containing carbon paste electrode for glucose biosensor application. J. Nanosci. Nanotechnol. 13(1):98-104.

Kim D.H., Nikles D.E., Johnson D.T. and Brazel C.S., 2008. Heat generation of aqueously dispersed CoFe2O4 nanoparticles as heating agents for magnetically activated drug delivery and hyperthermia. J. Magn. Magn. Mater. 320:2390-2396.

Kita E., Oda T., Kayano T., Sato S., Minagawa M., Yanagihara H., Kishimotol M., Mitsumata C., Hashimoto S., Yamada K. and Ohkohchi N., 2010. Ferromagnetic nanoparticles for magnetic hyperthermia and thermoablation therapy. J. Phys. D: Appl. Phys. 43:474011(9pp).

Kumar M., Gurpal S.,Vikas A., Sujeet M., Uma S., Jagannathan N.R., Sameer S., Amit K.D.. Surender K. and Harpal S., 2012. Cellular interaction of folic acid conjugated superparamagnetic iron oxide nanoparticles and its use as contrast agent for targeted magnetic imaging of tumor cells. Intl. J. Nanomed. 7:3503–3516.

Miao G., Chailu Q., Chen H.W., Xiao Z.L., Husheng Y. and Keliang L. 2011. Multifunctional superparamagnetic nanocarriers with folate-mediated and pH- responsive targeting properties for anticancer drug delivery. Biomaterials 32:185-194.

Morteza M., S. Sant, B. Wang, S. Laurent, Tapas S., 2011.Superparamagnetic iron oxide nanoparticles (SPIONs): Development, surface modification and applications in chemotherapy Adv. Drug Deliv. Rev. 63:24-26.

Mosmann T., 1983. Rapid colorimetric assay for cellular growth and survival: application to proliferation and cytotoxicity assays. J. Immunol. Meth. 65:55-63.

Nikki P., Mary J.T., Elaine W., JeVrey D.L., Philip S.L. and Christopher P. L., 2005. Folate receptor expression in carcinomas and normal tissues determined by a quantitative radioligand binding assay. Anal. Biochem. 338:284-293.

Prasad A.I., Parchur A.K., Juluri R.R., Jadhav N., Pandey B.N., Ningthoujam R.S. and Vatsa R.K., 2013. Bi-functional properties of Fe3O4@YPO4:Eu hybrid nanoparticles: hyperthermia application. Dalton Trans. 42:4885-4896.

R. W. Silverstein, F. X. Webster, D.J. Kiemle, Spectrometric identification of organic compounds, seventh ed., John Wiley & Sons, Inc., New Jersey, 2005.

R.T. Gordon, J.R. Hines, D. Gordon, 1979. A biophysical approach to cancer treatment via Intracellular temperature and biophysical alterations. Med. Hypotheses 5:83-102.

Rabin Y., 2002. Is intracellular hyperthermia superior to extracellular hyperthermia in the thermal sense. Int. J. Hyperthermia 18:194-202.

Raghumani S.N., Vatsa R.K., Kumar A., Pandey B.N., in: S. Banerjee, A. K. Tyagi (Eds.), Functionalized magnetic nanoparticles: concepts, synthesis and applications in cancer hyperthermia, Elsevier Inc. London, 2012, pp.229-260

Rohidas B.A., Soon K.H., Hwang T.L., Tae H.K., Dhananjay J., Hu L.J., You K.K., Myung H.C. and Chong S.C., 2010. The therapeutic efficiency of FP-PEA/TAM67 gene complexes via folate receptor-mediated endocytosis in a xenograft mice model Biomaterials 31:2435-2445.

Rosensweig R.E., 2002. Heating magnetic fluid with alternating magnetic field. J. Magn. Magn. Mater. 252:370-374.

Rui H., Ruijun X., Zhichuan Xu , Yanglong H., Song G. and Shouheng S. 2010. Synthesis, functionalization and biomedical applications of multifunctional magnetic nanoparticles. Adv. Mater., 22:2729–2742

Runa G., Lina P, Priyabala D.Y., Meena S.S., Tewari R., Kumar A., Sharma S., Gajbhiye N.S., Pandey B.N., Raghumani S.N., 2011. J. Mater. Chem. 21:13388-13398.

Sonali S., Deepthy M., Adersh A., Shantikumar N. and Manzoor K., 2010. Folate receptor targeted, rare-earth oxide nanocrystals for bi-modal fluorescence and magnetic imaging of cancer cells. Biomaterials 31:714-729.

Stanger O., 2002. Physiology of folic acid in health and disease. Curr. Drug Metab. 3:211-223.

Steven D.W., Richard H.L., Leslie R.C., Daniel W.F., Verna F., Vincent R.Z. Jr. and Barton A.K, 1992. Distribution of the folate receptor gp38 in normal and malignant cell lines and tissues. Cancer Res. 52:3396-3401.

Veronica I.S., Thomas R.P. and Sungho J. 2009. Magnetic nanoparticles for theragnostics. Adv Drug Deliv Rev. 61(6):467–477

Zhang L.Y., Gu H.C. and Wang X.M., 2007. Magnetite ferrofluid with high specific absorption rate for application in hyperthermia. J. Magn. Magn. Mater. 311:228-233.